Int J Adv Manuf Technol (2007) 35:127–134
DOI 10.1007/s00170-006-0703-3

ORIGINAL ARTICLE

Automatic inspection of the width and gap of etching transistors in TFT-LCD panels using sub-pixel accuracy estimation

Chern-Sheng Lin · Chia-Wen Tsai · Ying-Cherng Lu · Chingfu Tsou · Su-Chi Chang

Received: 20 January 2006 / Accepted: 16 June 2006 / Published online: 21 September 2006

Abstract In this paper, the width and gap of etching transistors in TFT-LCD panels were measured using sub-pixel accuracy estimation, and the accuracy was tested in a noisy environment. The concept of line width measurement was introduced in terms of line distance and defect measurement based on the low and high spatial frequency distribution change of TFT-LCD panel image. Some patterns do not need to have the line width and distance measured, while others have different measurement requirements. The conductor border of a pattern is normally an area with a flat change of grey scale, but we are still able to find an accurate measurement with the proposed method. In the TFT-LCD testing pattern, there are circular etching structures, and for measurement we focus on the position of the center of the circle and the size of the radius. This method can be used quickly and accurately for measuring the TFT short, ITO open, marking, spot particle or scratching on the panel caused by over etching.

Keywords TFT-LCD panel · Sub-pixel accuracy · Noisy environment

1 Introduction

This study focuses on the TFT (thin film transistor) position and relevant measurement during the array part of the TFT-LCD (liquid crystal display) manufacturing process when conducting tessellation after repeated coating, coating photo-resisting, etching, lithography, exposure, photo-resist stripping and removal to identify the central position of the TFT for processing at a later stage.

The most common problem of under-etching found during TFT-LCD etching is TFT open, ITO open or data open; and the longer the etching liquid remains on the glass substrate, the clearer the under-etching appears to be. Serious under-etching problems will result in the failure to make a fine even width conductor, where as over-etching will cause short circuits. In response to the demand for lower manufacturing costs and higher yield rates, it is necessary to develop better etching technology. Moreover, the time spent on failures (such as short circuits) needs to be further reduced to prevent rising production costs and poor quality [1–4].

The connection between image information and the background of the margin is the changeable high frequency data [5]. This can be observed by reviewing color distribution after defining the width for measurement. The image has progressive characteristics and the presentation of one line shows one crest and two troughs in fine change. Fine change often results in irregular shaping that relies on a selective system for screening the defects which are caused by the environment or etching process.

C.-S. Lin (✉) · C.-W. Tsai · C. Tsou · S.-C. Chang
Department of Automatic Control Engineering,
Feng Chia University,
Taichung, Taiwan
e-mail: lincs@fcu.edu.tw

Y.-C. Lu
Metal Industries Research and Development Centre,
Kaohsiung, Taiwan

2 Measurement method

This paper estimated the characteristic image changes between high and low frequencies. It also considered the adoption of a different slope to locate two troughs first and then measure the linear width scope with sub-pixel technology [6, 7]. Figure 1 shows the line width measuring

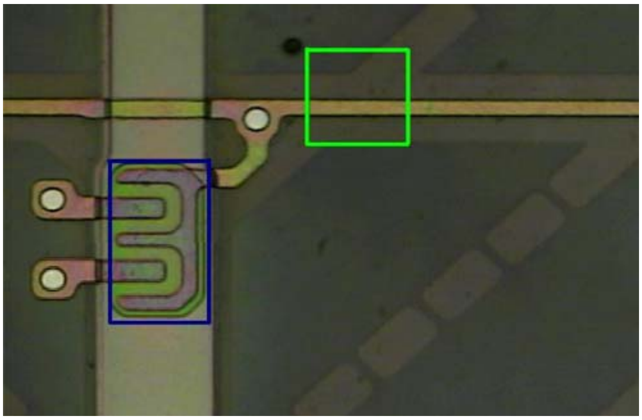

Fig. 1 Measuring area of line width

scope (green border lines) and results; Fig. 2 is the color strength distribution of the line adjacent area with a line width of 14.342 pixels, and Fig. 3 indicates the line width algorithm, where the X axis refers to the vertical length of the line width measuring the area of Fig. 2 in pixel units and the Y axis is the change of grey-scale vertical position resolution in the measuring area. We assume the measuring area is 100×120 and the progressive change of grey scale is 120 pixels; the same measurements were applied 100 times to the horizontal direction in order to obtain the average value.

The two coordinates in Fig. 3 show the change of the surrounding image line width depth of the etching circuit along with the frequency change of the coordinate, where W is the line width to be measured. By taking advantage of the fine change in high and low frequencies, we are able to define the location of the borders and the size of the line width. The threshold value is introduced to locate Point A1 and A2. We are able to identify B1, B2, C1, and C2 with different slopes in the adjacent area in the same direction. The slope is obtained through the relationship shown in Fig. 4; because a_i,i=1$\cdots n$ has a width of 1 pixel. The equation is simplified as eq. (1), where c is the starting central position with the plus parameter on the right and the minus parameter on the left in function (f).

$$m_i = \tan\left(\frac{b_i}{a_i}\right) = \tan\{f(c \pm i) - f[c \pm (i-1)]\} \quad i = 1 \cdots n \tag{1}$$

In order to acquire more precise B1 and B2 measurements, we assume that there is a normal distribution of Area I and II in Fig. 4, or we are able to make use of polynomial regression to assume color depth (h) as function ^{n} of coordinate (y). The equation is conveyed as eq. (2):

$$\hat{h} = k_n y^n + k_{n-1} y^{n-1} + \cdots + k_2 y^2 + k_1 y + k_0 \tag{2}$$

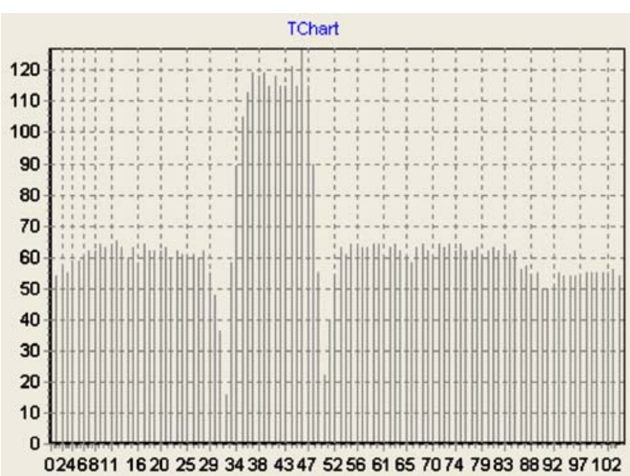

Fig. 2 Gray scale distribution of line width

Assuming S is the square sum of deviation and eq. (3):

$$S = \sum_{i=1}^{m}\left(h_i - \hat{h}_i\right)^2 = \sum_{i=1}^{m}\left(y_i - \left(k_n y^n + k_{n-1} y^{n-1} + \cdots + k_2 y^2 + k_1 y + k_0\right)\right)^2 \tag{3}$$

From a partial differential equation of k_0,k_1,$\cdots\cdots$,k_n to acquire

$$\frac{\delta S}{\delta k_i} = 0 \quad i = 1 \cdots n$$

The proximity matrix relationship is found as eq. (4):

$$\begin{bmatrix} m & \sum y_i & \cdots & \sum y_i^n \\ \sum y_i & \sum y_i^2 & \cdots & \sum y_i^{n+1} \\ \sum y_i^2 & \sum y_i^3 & \cdots & \sum y_i^{n+2} \\ \vdots & \vdots & \vdots & \vdots \\ \sum y_i^n & \sum y_i^{n+1} & \cdots & \sum y_i^{2n} \end{bmatrix} \begin{bmatrix} k_0 \\ k_1 \\ k_2 \\ \vdots \\ k_n \end{bmatrix} = \begin{bmatrix} \sum h_i \\ \sum y_i h_i \\ \sum y_i^2 h_i \\ \vdots \\ \sum y_i^n h_i \end{bmatrix} \tag{4}$$

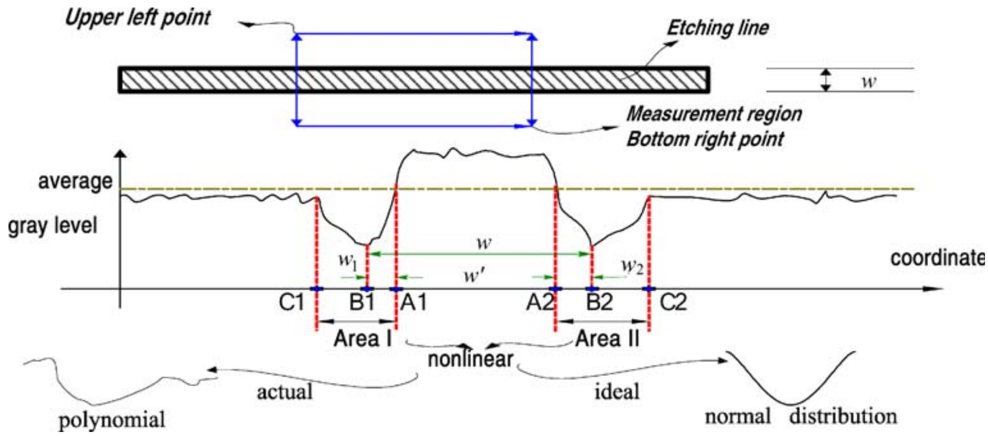

Fig. 3 Change of the line width depth of the etching circuit along with the coordinate variations

Finally, Gaussian Elimination or the Gaussian–Jordan Method is adopted to find the solution for $k_0, k_1, \cdots\cdots, k_n$; as well as obtain an approximation curve equation and locate the area for minimum value through the differential equation. Thus, we find the value of Δw_1 and Δw_2; $W = w' + \Delta w_1 + \Delta w_2$ to enable the accuracy of line width resolution to be lower than that of one pixel.

The same concept of line width measurement has been introduced in terms of line distance and CDLOSS measurement based on the low and high spatial frequency distribution change in image. Some patterns need to have the line width measurement and distance and others have different measurement requirements. After distinguishing this type of pattern, this system adopts the measurement of the certain pattern. Figure 5 describes the measurement of line distance and CDLOSS: W_1, W_2, and W_3 are line widths to be measured and D_1 and D_2 are line distances to be measured. The equation is shown as follows:

$$W_{i+1} = A_{2i+2} - A_{2i+1} \qquad i = 0, 1, 2$$

$$D_i = A_{2i+1} - A_{2i} \qquad i = 1, 2$$

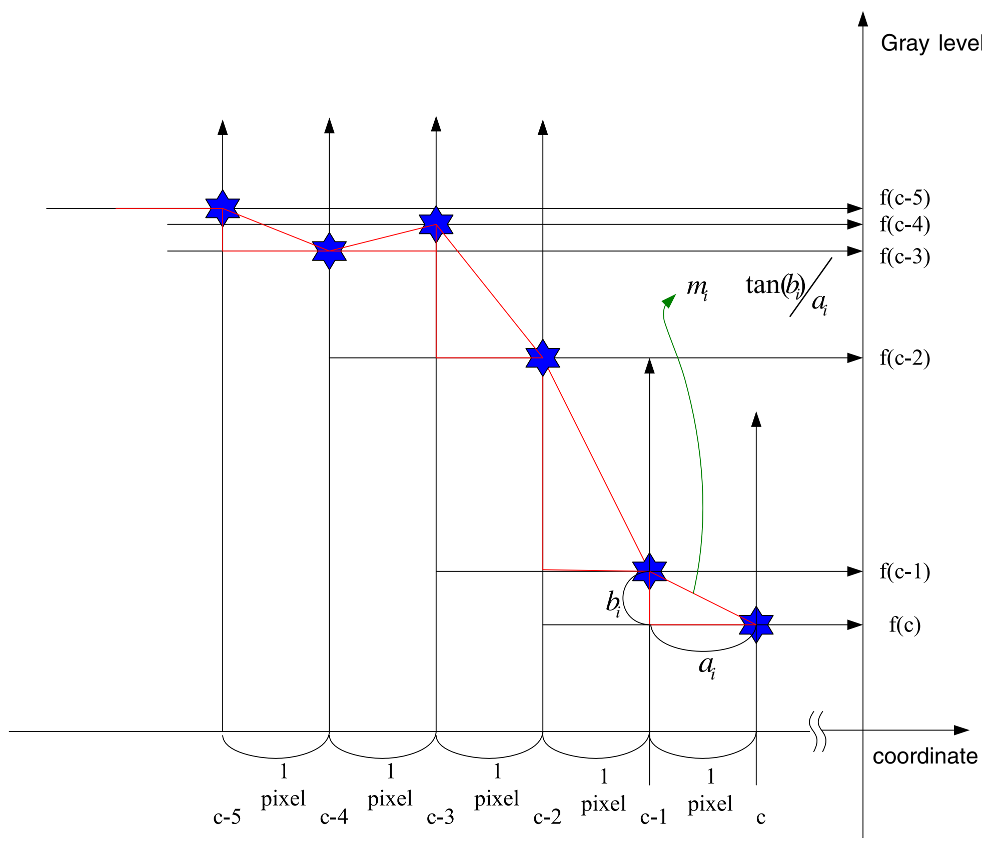

Fig. 4 Simplified algorithm of slope rate (left and right in symmetry)

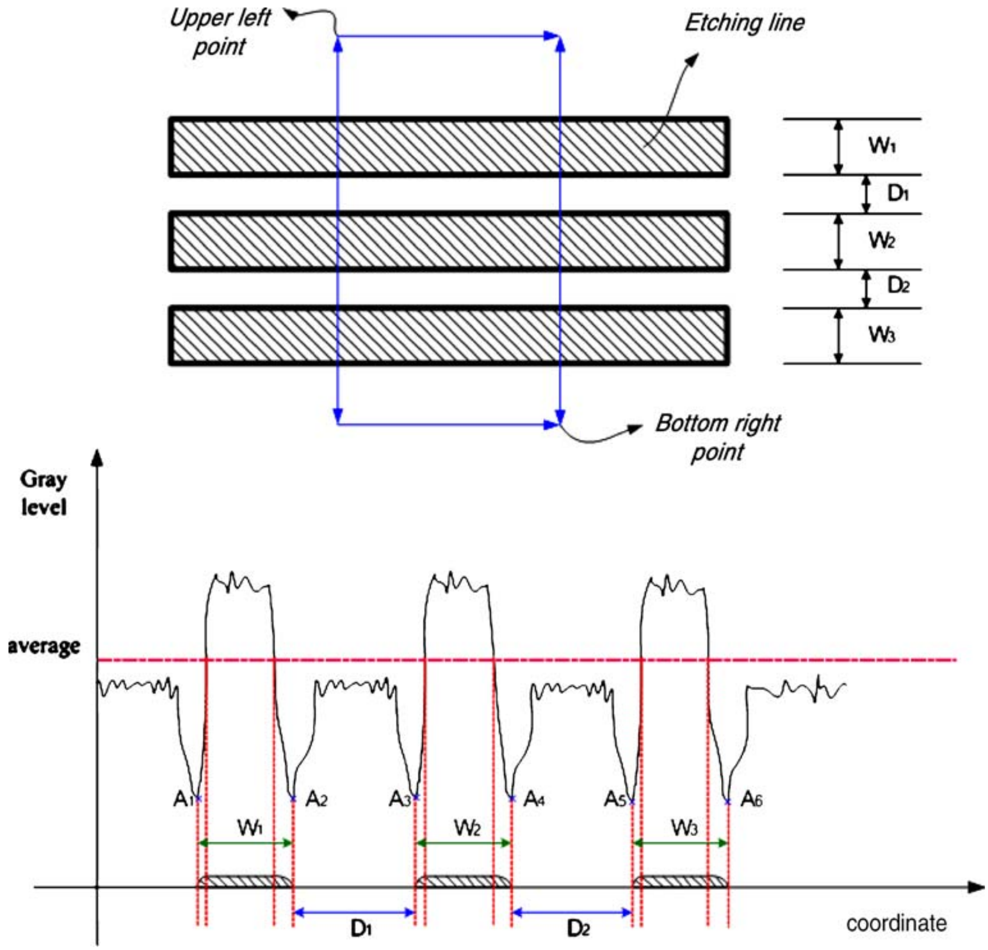

Fig. 5 Measurement of line distance and CDLOSS

The measurements of the border distance and structural size of the TFT of two random circuit layout lines on the board are selected for the measurement of horizontal and vertical lines. Under micro-imaging observation, a fine conductor will change by a certain degree during the manufacturing of TFT and etching circuits. To reduce errors while taking the measurements, we took a full range of measurements and calculated the mean. The conductor border of a pattern is normally an area showing a flat change of grey scale, so if the measurement result is obtained from the original image, it is difficult to obtain an accurate measurement when the change in the border is not significant. To enhance the image contrast, we first used the average filter and Robert Method to conduct an initial strengthening of the image.

The average filter, also called the low pass filter, enables a smooth transition of signals by enhancing the smooth part (singles of low frequency) and controlling the part in dramatic transition (signals of high frequency). The Roberts' edge detector is used to strengthen smooth images in order to obtain sharp contrast of one border before using an image with border information to conduct measurements.

Mask design in Roberts' edge detector are $\begin{bmatrix} 0 & 1 \\ -1 & 0 \end{bmatrix}$ and $\begin{bmatrix} -1 & 0 \\ 0 & 1 \end{bmatrix}$ or $\begin{bmatrix} -1 & 0 & 0 \\ 0 & 0 & 0 \\ 0 & 0 & 1 \end{bmatrix}$ and $\begin{bmatrix} 0 & 0 & 1 \\ 0 & 0 & 0 \\ -1 & 0 & 0 \end{bmatrix}$.

Here we adopt the first operator in each pair because it is very quick and particular sensitive to edges that run diagonally from the lower part to the upper part. When measuring the horizontal line, we use the estimation of minimum square to assume coordinate y equals the function of coordinate x [1]: $y=k_1x+k_0$. From the above equation, we obtained n=1 and eq. (5)

$$\begin{bmatrix} m & \sum x_i \\ \sum x_i & \sum x_i^2 \end{bmatrix} \begin{bmatrix} k_0 \\ k_1 \end{bmatrix} = \begin{bmatrix} \sum y_i \\ \sum x_i y_i \end{bmatrix} \tag{5}$$

From eq. (5), we obtained k_0, k_1 and $y=k_1x+k_0$. The regression equation of this measured line is the same method applied to the measurement of a vertical line. When two line equations are defined, we are able to use the relationship between connecting points and normal form to define the vertical distance of two lines.

The innovative aspects of the measurements of the slope line, shown in Fig. 6, are applied to define the shortest distance of two horizontal lines in each degree. Similarly, the pre-treatment of images and the calculation of line equations are based on those used in horizontal and vertical measurement or with the polynomial regression method to acquire k_0, k_1 and then $y=k_1x+k_0$, which is the equation of line $\overline{R_1R_2}$. The shortest distance, D, between L2 and L1, can even form a circle by using any point, Rv, on L2 as the center and D is the radius. The circle connects L1 on Point R and $\overline{R_vR}\perp\overline{R_1R_2}$. Let us assume:

$$\begin{aligned}\overline{R_1R_2} &= \langle X_1, Y_1\rangle + r\bullet\langle X_2 - X_1, Y_2 - Y_1\rangle \\ &= \langle X_1 + r\bullet(X_2 - X_1), Y_1 + r\bullet(Y_2 - Y_1)\rangle\end{aligned}$$

The distance between Rv and $\overline{R_1R_2}$ is $D(r)$ or is shown as eq. (6)

$$\left(R_V \to \overline{R_1R_2}\right), D(r) = \sqrt{\left(X - X_p\right)^2 + \left(Y - Y_p\right)^2} \tag{6}$$

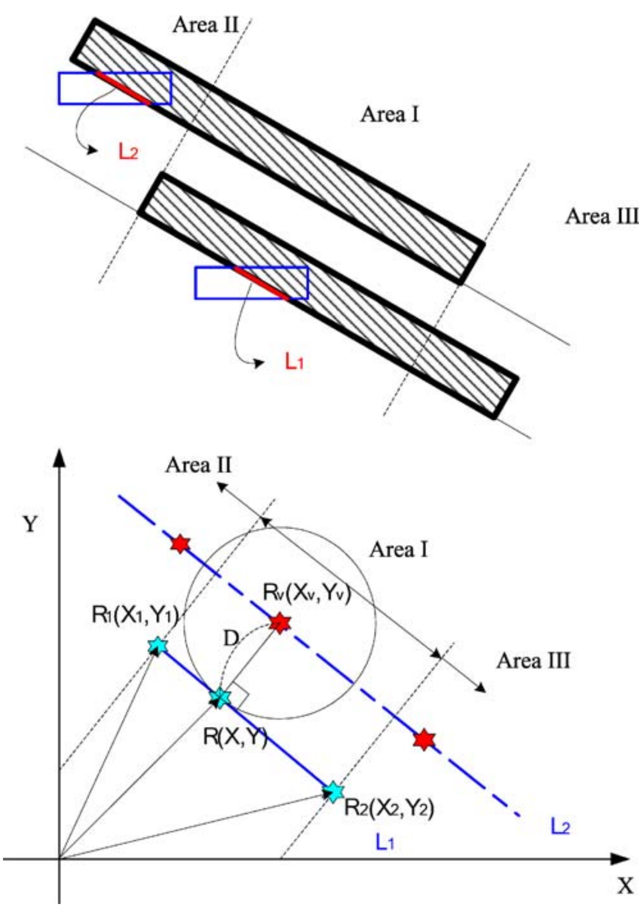

Fig. 6 Slope measurement

Table 1 Search results for measurement errors

Item	Pattern 1	Pattern 2	Pattern 3	Pattern 4
Average error to original (pixels)	1.4635	2.0249	1.5455	2.1152
Measurement errors (μm)	0.292696	0.40497	0.30909	0.42304

From eq. (6), we acquire eq. (7)

$$\begin{aligned}D^2(r) &= (X - X_p)^2 + (Y - Y_p)^2 \\ &= [(X_1 + r\bullet(X_2 - X_1) - X_p]^2 + [Y_1 + r\bullet(Y_2 - Y_1) - Y_p]^2\end{aligned} \tag{7}$$

Assume the distance from Rv to $\overline{R_1R_2}$ is 0 as in eq. (8)

$$if\ \frac{d}{dt}D^2(r) \to 0 \tag{8}$$

Simplified eq. (8) is as follows

$$\begin{aligned}&2\{[X_1 + r\bullet(X_2 - X_1) - X_v](X_2 - X_1) \\ &+[Y_1 + r\bullet(Y_2 - Y_1) - Y_v](Y_2 - Y_1)\} = 0\end{aligned}$$

We then acquire r in eq. (9)

$$r = \frac{(X_1 - X_v)(X_1 - X_2) + \left(Y_1 - Y_p\right)(Y_1 - Y_2)}{(X_2 - X_1)^2 + (Y_2 - Y_1)^2} \tag{9}$$

The value of r refers to its position in the area range. That is, if R is located in area II, the range of R in area I and III shall be between 0~1 to satisfy the requirement. If R is not in the range, it means that R is outside the shadow range of $\overline{R_1R_2}$. To put $\overline{R_1R_2}$ back, it must be able to satisfy the requirement in eq. (10):

$$\begin{cases} if\ r < 0\ then\ r = 0 \\ if\ r > 0\ then\ r = 1 \end{cases} \tag{10}$$

After positioning R, we are able to acquire the shortest distance of vertical $\overline{R_1R_2}$, D.

Table 2 The size and ratio of the test patterns

Item	Pattern Size	Width Ratio
Pattern 1	118×141	0.184
Pattern 2	144×244	0.225
Pattern 3	130×232	0.203
Pattern 4	117×133	0.183

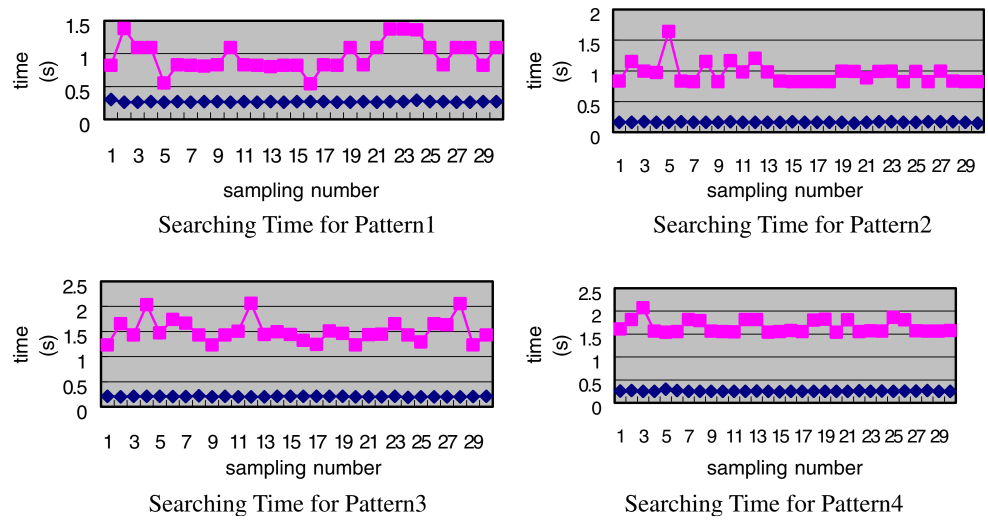

Fig. 7 Results of pattern searching time(!!!:line width, :gap)

3 Experimental results

In the TFT-LCD testing pattern, there exists circular etching structures, and for measurement we focus on the position of the center of the circle and the size of the radius. With image border information, the connecting point of the perpendicular line of two lines composed of any three different points on circumference will pass the center of the circle.

Experimental data in Table 1 indicate the desired searching pattern and the pattern being actually found. If we estimate the result without considering the type of pattern, there are about 120 data points found with the original error of the different pattern centers with an average value of 1.789 pixels in reflection to 0.000358 mm, about 0.358 μm. With less than 1 μm of overall accuracy error, it is sufficient for the discussion of pattern recognition as well as application of on-line inquiry.

Through good characteristic description design, these searches and contrasts will not be influenced by external factors such as etching quality, noise, spot, and optical field to there by affect the recognition rate. In addition, the processing rate during contrast is another interesting consideration for on-line operational system testing. The subjects were pattern1~pattern4, as shown in Table 2. Thirty individual samples were collected from each pattern. The initial value of parameter similarity was set as 75. Thirty records, for a total of 120, were kept during the search from the beginning to correct the central coordinate identification of each pattern. The pattern search result from beginning to end is shown as Fig. 7 with a single period indicated by the blue line and the continuous period in red.

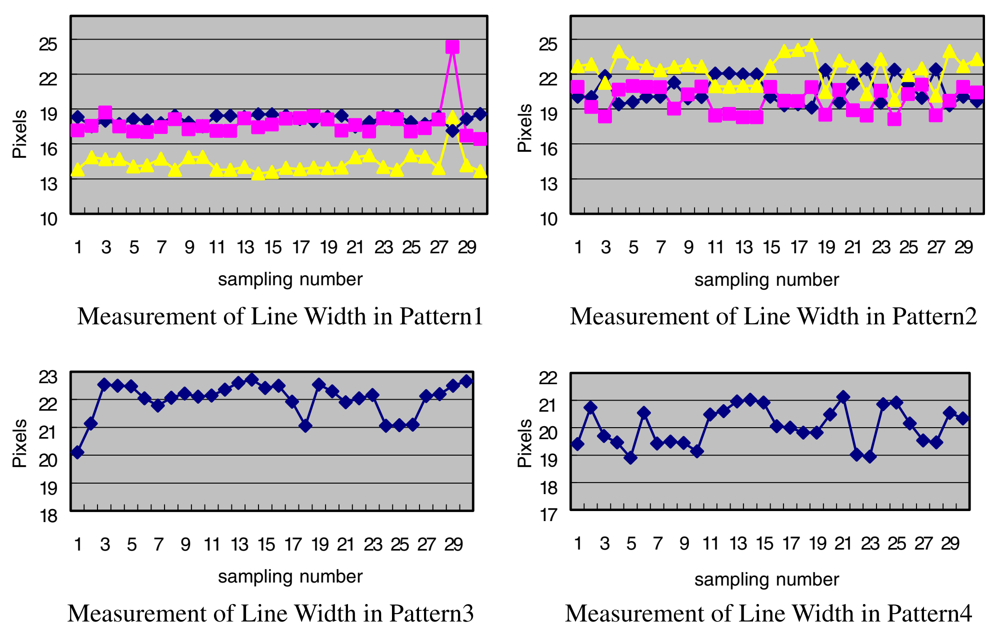

Fig. 8 Distribution of the measuring results of line width measurement of pattern(!!!:line width, :gap 1, Δgape 2)

Fig. 9 Results of automatic measurement

Measurement of Line Width of Pattern1 (Center:"220.5, 282") Width:0.003863mm , Line Distance :0.003432 and 0.00256)

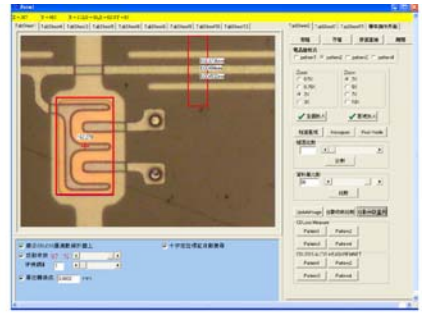

Measurement of Line Width Pattern2 (Center:"162, 278") (Line Width:0.00404mm, Line Distance :0.003736 and 0.004532)

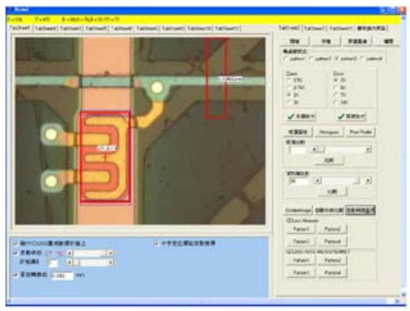

Measurement of Line Width of Pattern3 (Center:"231, 307.5") (Line Width:0.004692mm)

Measurement of Line Width Pattern4 (Center:"199.5, 235") (Line Width:0.003984mm)

Fig. 10 Results of manual measurement

Horizontal Measurement (0.0156mm)

Vertical Measurement (0.0034mm)

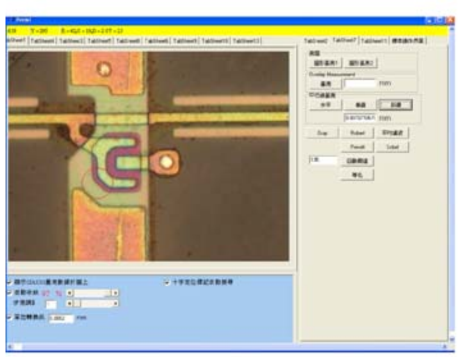

Slope Measurement (0.0071mm)

Circular Measurement (Radius:0.00336mm , Center of the Circle:"361.258 , 253.579")

When the panel enters the production line in the measurement operational procedure, the system first automatically identifies the central coordinate of the corresponding pattern and then the line width and distance. The panel shall belong to one of patterns 1~4. The value measurement of pattern 1 and pattern 2 shall have one for line width and two for line distance; pattern 3 and pattern 4 are required to have one measurement value of line width.

Due to the steep slope occurring on the wide border of the fine conductor during the manufacturing of the TFT-LCD panel, the value of each measurement refers to that of one full range showing the 30 records of each pattern measurement. The distribution of the measuring results of each pattern is shown in Fig. 8.

The average line width, distance, and pixel length of pattern 1 are 18.091, 17.791 and 14.353, respectively, and for pattern 2 are 20.606, 19.755 and 22.339. The line widths of pattern 3 and pattern 4 are 22.011 pixels and 20.043 pixels. Each pixel has the corresponding actual physical quantity of 0.2 μm. In this nano accuracy measurement, an error may exist in a few pixels to reflect a minor error of the manufacturing quality of the fine conductor for further manufacturing reference.

4 Discussion and conclusion

The aim of this research was to develop an automatic testing TFT-LCD etching system and to test the effectiveness and stability of the system. A total testing was conducted in real-time operation, showing satisfactory performance, as indicated in Figs. 9 and 10.

When the TFT-LCD is sent to test the lens, the system identifies a marked image of cross coating and automatically jumps to the mode of cross-positioned coating for processing. The positioned cross-center information and adjusted angle is used as the original point for coordinate reference calibration. Next, the automatic image mode traces to identify the central position of the TFT and passes a service agent to transfer this TDT to the testing screen center for automatic measurement of line width and distance, as shown in Fig. 9. Finally, the measurement results of the TFT central position line width and line distance are shown in the record form at the right bottom and the above-mentioned moves are automatically done without any labor interruption.

Some measurements, due to requirements, are not done completely automatically, but are partly manual to check etching quality, relative position, and double image on the fine component structure of the panel to identify causes of poor etching to improve the future manufacturing processes. For example, Fig. 10 includes the main menu of the manual measurement mode of the horizontal distance, vertical distance, and random slope distance of any two etching circuit border lines and TFT structure to decide the overlapping size of any two lines in symmetrical border and the information of radius size and the center of a circle acquired by the measurement of circular components.

The complicated TFT-LCD manufacturing requires more detailed testing; and due to higher demand for panel size, the system also needs more improvement in testing speed, accuracy, stability, and functionality. This study can help improve inspection of TFT and categorize the defects to be tested for the occurrence of TFT short, ITO open, marking, spot particle or scratching on the panel caused by over-etching.

Acknowledgments This work was sponsored by the Taiwan National Science Council under grant number NSC 94-2212-E-035-001 and by the MIRDC under grant number 92-EC-17-A-04-R7-0180.

References

1. Lin CS, Lay YL, Huan CC, Chang HC, Hwang TS (2003) An image-based LCD positioning system utilizing the modified FHT method. Optik 114(4):151–160
2. Alexander BF, Ng KC (1991) Elimination of systematic error in sub-pixel accuracy centroid estimation. Opt Eng 30:1320–1331
3. Sokolov SM, Treskunov AS (1992) Automatic vision system for final test of liquid crystal displays. International Conference on Robotics and Automation, France 1578–1582
4. Cho J, Lin CS, Jan BJ, Lin CH, Chang NC (2005) An opto-electrical method for measuring the gap of LCD glass plates. Opt Laser Technol 37(8):623–630
5. Lin CS, Wu CY, Hsu HC, Li KMC, Lin L (2004) Rapid bio-test strips reader with image processing technology. Optik 115(8):363–369
6. Jing X, Chau LP (2004) An efficient three-step search algorithm for block motion estimation. IEEE Trans Multimedia 6(3):435–438
7. Murase H, Vinod VV (2000) Fast visual search using focuded color matching-active search. Syst Comput Jpn 31(9):81–88